Supporting Information

A bifunctional auxiliary electrode for safe lithium metal batteries

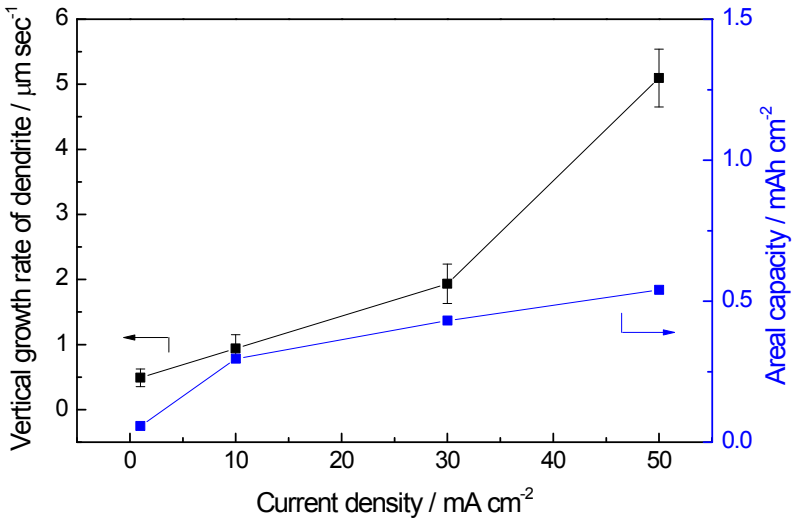

Figure S1. Vertical growth rate of dendrite at various current densities. The black and blue lines represented vertical growth rate of dendrite and areal capacity, respectively

This experiment was conducted in sandwich cell. The piece of lithium foil was first pressed onto the case part of the cell and cover by customized PVDF rings (outer diameter = 16.5 mm, inner diameter = 8 mm, thickness = 100 μm). The electrolyte was dropped on the surface of lithium. Finally, the second lithium foil was plated on top of the customized PVDF. The whole cell was assembled in an Ar-filled glovebox using a CR2032-type coin cell with 300 μm thick Li foil. The estimate of vertical growth rate, with respect to the planar growth in the inner site of customizes PVDF rings, was possible by checking the time required for short-circuiting involving sudden voltage drops.

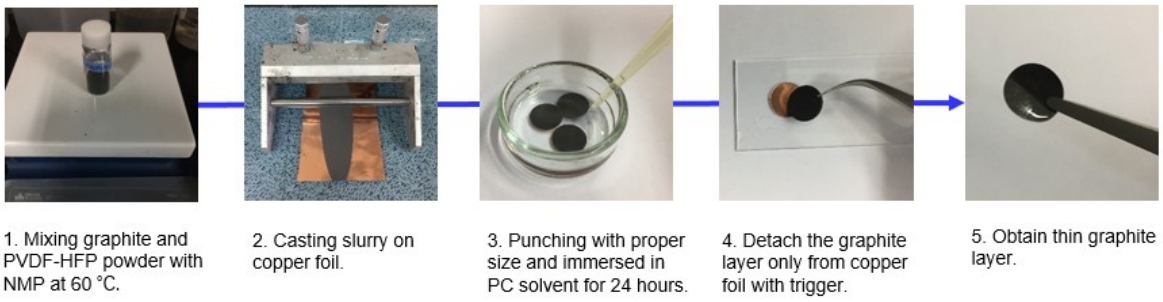

Figure S2. Fabrication processes of a thin graphite layer are described step by step.

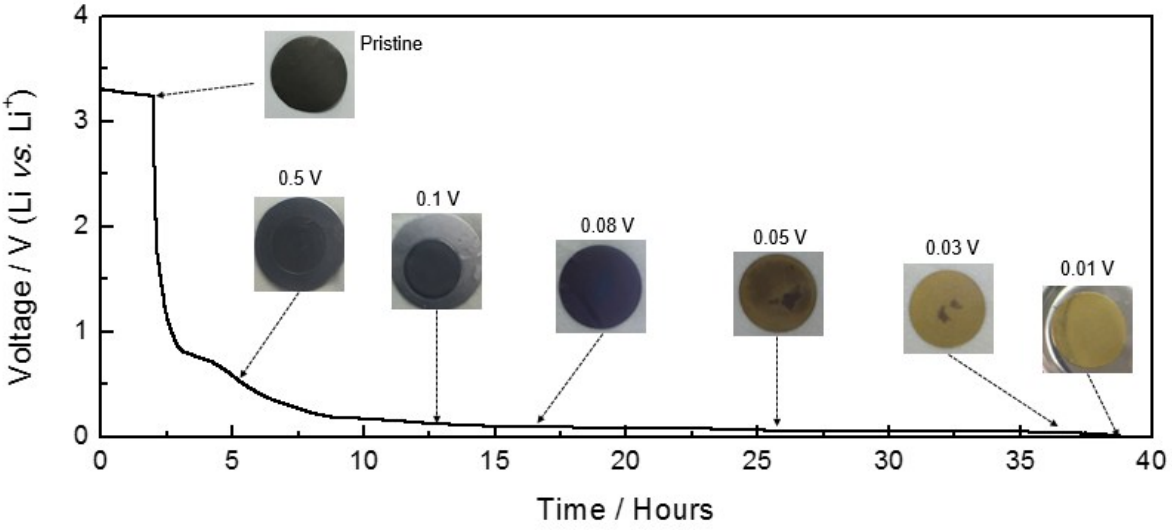

Figure S3. Typical potential profile of a graphite layer with color change of graphite by lithiation. The pristine graphite layer that is fully de-lithiated is black in color. The color of graphite layer becomes yellow with lithiation. Each cell was discharged with a current density of 10 mA g^{-1} to its cut-off voltage and disassembled to obtain graphite images.

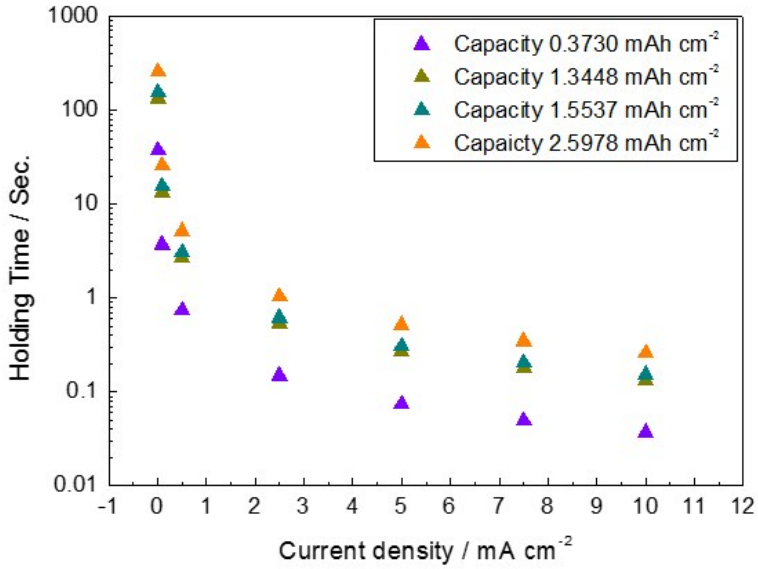

Figure S4. The delay time that can suppress the growth of lithium dendrite depending on the current density. The larger the capacity of the auxiliary electrode, the longer the allowable dendrite growth delay time.

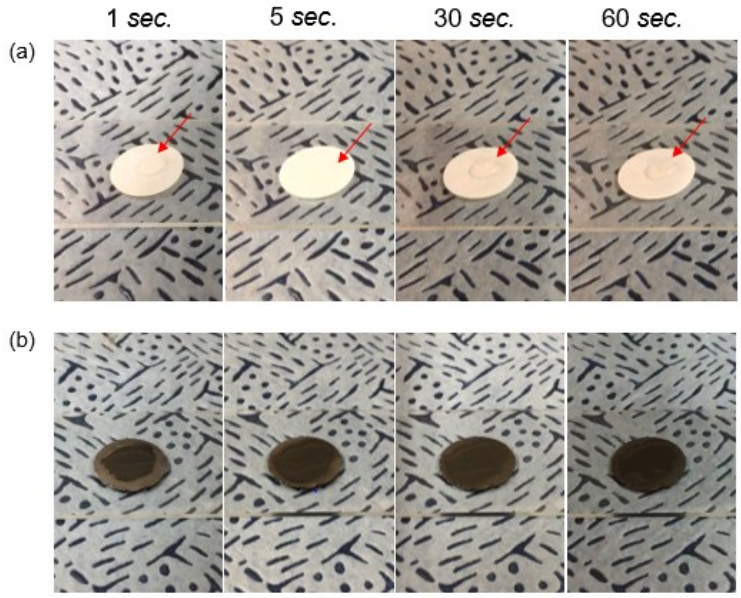

Figure S5. Images showing the contact angle of dropped electrolyte on (a) separator and (b) an auxiliary graphite layer. The electrolyte on the separator maintains a high contact angle for up to 60 seconds. Conversely, as soon as the electrolyte was dropped onto the graphite layer, it penetrated the graphite layer.

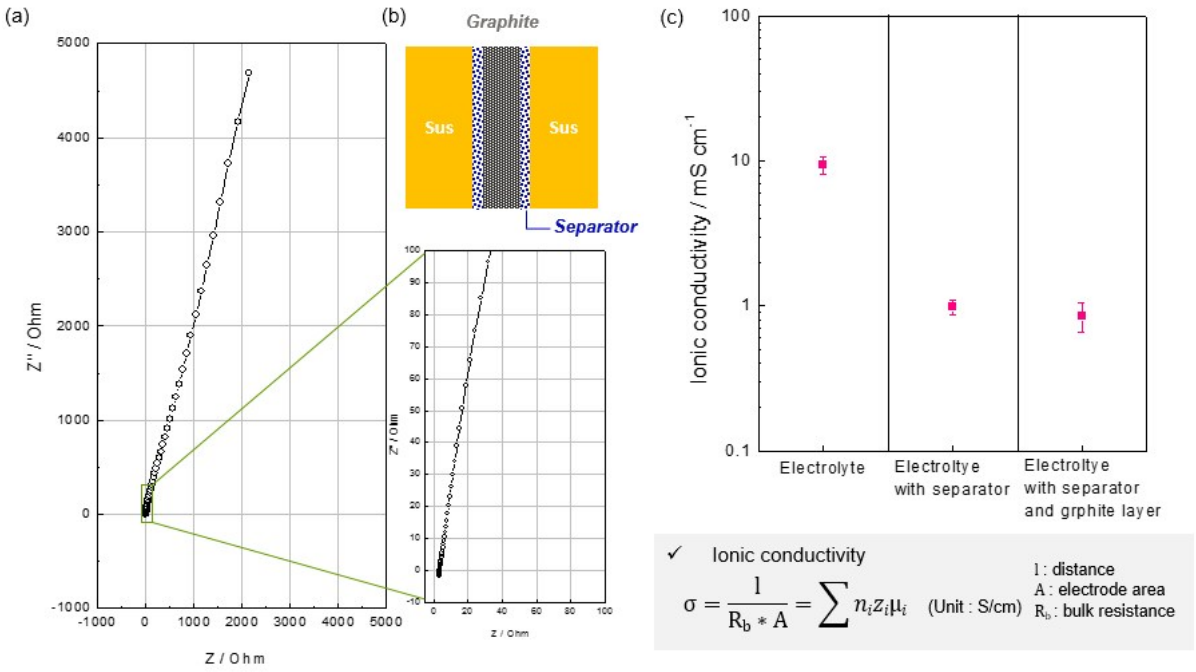

Figure S6. (a) Nyquist plot of a SUS-SUS symmetric cell with a graphite layer between the plates. (b) A schematic illustration of the cell configuration to measure EIS. Due to the electronic conductivity of the graphite layer, two separator sheets on each side were used to block the electronic path. (c) Ionic conductivity is measured in various cell configurations to determine the effect of each component.

The intercept of the x-axis generally represents bulk resistance, which is mainly influenced by ionic conductivity. In this system, the distance (l) and area (A) are set to the component thickness between the two stainless steel substrates and the area of the stainless steel substrate, respectively. Thus, the bulk resistance can be converted into ionic conductivity using the equation in figure S6. To measure the conductivity of the pure electrolyte, a constant distance and area are fixed between two SUS plates by inserting a donut type Teflon ring. Figure 6c shows the ionic conductivity in three different cases. The ionic conductivity of the pure electrolyte was approximately 10 mS cm^{-1}, which is consistent with previous reports. (Journal

of Power Sources, 196, 9743-9750, 2011). Additional conductivity measurements were performed with and without graphite layers between the separators to determine the effect of only the thin graphite layer located between the separators on the ionic conductivity. The presence of separator result in a lower ionic conductivy (0.98 mS cm^{-1}) due to its low porosity, which inhibited the movement of lithium ions through the separator. However, an additonal thin graphite layer inserted between two separators did not seem to significanlly affect the Li ion mobility (0.86 mS cm^{-1}).

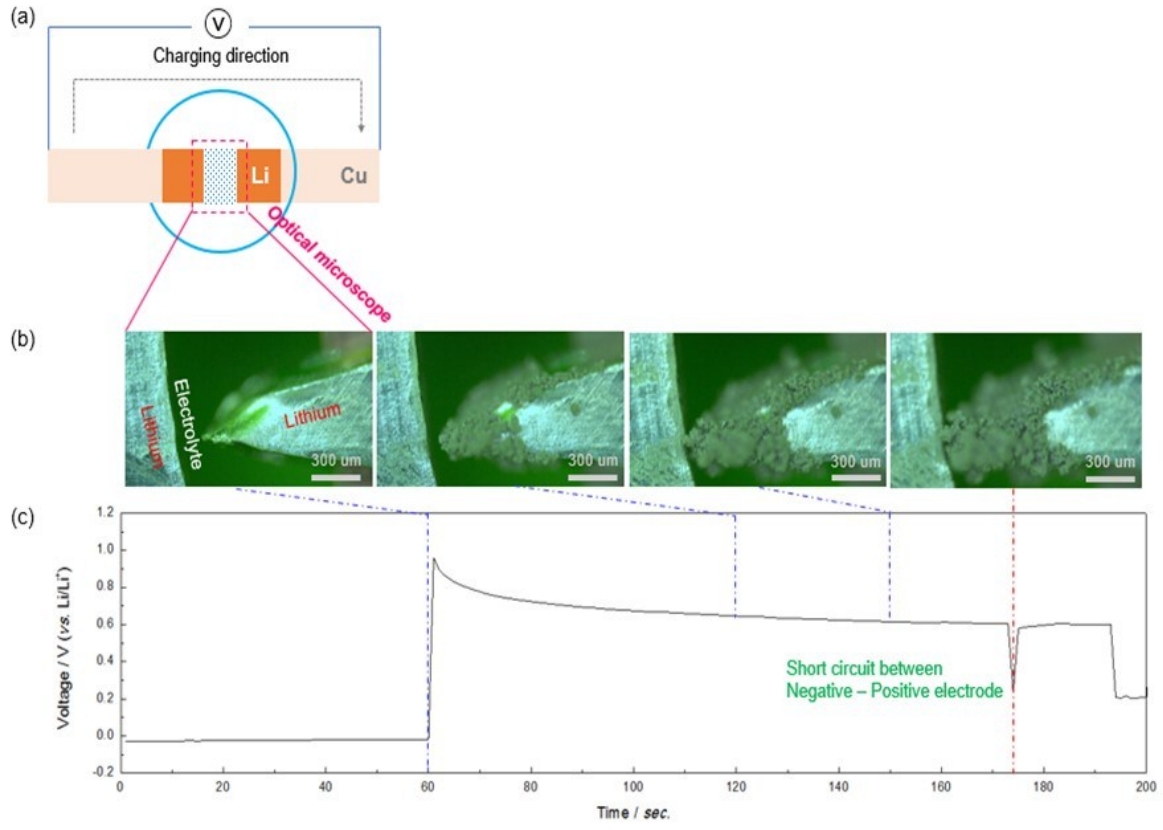

Figure S7. (a) A schematic illustration of cell configuration for *in-situ* optical measurement. (b) Optical microscopy images of the Li-Li symmetric cell were taken in galvanostatic mode. (c) Potential curve of Li-Li symmetric cell.

Two lithium metal slices were placed on both sides of the copper foil and electrodeposited with lithium in one direction. The initial voltage of between two electrodes was 0 V due to the symmetry of the cells. Once a current was applied, lithium ions were deposited on the lithium surface. The distance between the two lithium metals decreased due to the deposition of lithium metal as shown in Figure S7b. Finally, the growing lithium metal front contacted the opposite side lithium metal, causing sudden voltage drop. However, since a large amount of current momentarily flowed through the internal short-circuit, the voltage drop recovered immediately the circuit was disconnected. Continuous electrodeposition of lithium ions creates more dendritic circuits, resulting in a stable voltage drop considered an internal short circuit.

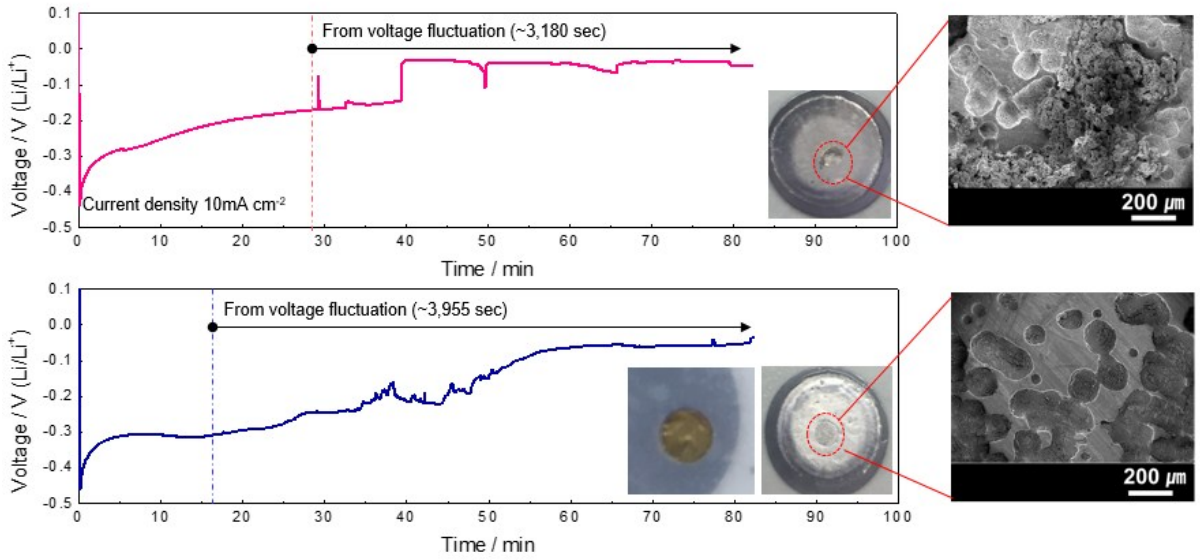

Figure S8. Typical potential profile and disassembly cell image of Li-Li symmetric cell (a) without a graphite auxiliary electrode (b) with a graphite auxiliary electrode.

The blockage of dendrite by an auxiliary electrode is further confirmed upon battery disassembly analysis. To induce the electroplating of lithium ions on the opposite electrode, we fabricate coin cells with a hollow area between two electrodes with no separators. For the

smart battery system containing an auxiliary electrode, the flexible graphite layer as auxiliary electrode was placed on the middle of the hollow area. Figure S8a presents a typical voltage profile of a Li-symmetric cell during the discharge process. At an initial stage, an activation energy of removal of oxide layer on lithium surface requires a higher over-potential, up to -0.45 V at 10 mA cm^{-2}. This over-potential converges with a gradual decrease. The first voltage fluctuation was detected after 29 min, indicating the connection of internal circuit by lithium dendrites. A constant current continued to flow for up to 83 minutes to form enough dendrite to be observed after the first detection. An identical experiment was carried out on cells with auxiliary electrodes (Figure S8b). The first voltage changes in this case were rather undistinguishable and were detected twice as fast because these voltage fluctuations come from not contact between negative and positive electrodes, but from the connection between lithium and auxiliary electrodes located at a half distance between negative and positive electrodes. To confirm the occurrence of short circuit, the lithium electrodes on the side from which lithium ions were extracted during the discharge process were obtained by disassembling each sample. Without an auxiliary electrode, black spots on the dendrites were visually observed and were clearly identified as lithium dendrites by SEM imagery. Not only numerous pores were seen on the lithium surface associated with lithium ion extraction sites, but also lithium deposition morphologies were also found. In contrast, the lithium surface obtained from the cell containing an auxiliary electrode was slightly darkish throughout the entire reaction zone, but had no black spots at all. Furthermore, only pores were observed on the lithium surface through the SEM photograph, while the graphite layer changed to yellow which indicating lithiation of the graphite. Based on the pore images and discoloration of graphite layer, it is inferred that additional lithium ions were not consumed by formation of lithium dendrite. It was consumed for reactions with the auxiliary electrode resulting in the blockage of hazardous dendrite growth.

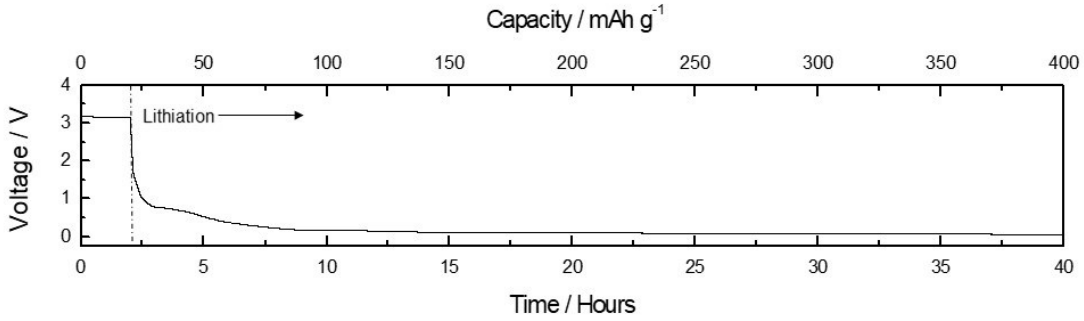

Figure S9. The voltage profile of the first discharge process of Li/Graphite (Auxiliary)/Graphite (Positive) cells with a 10 mA g^{-1} current density.

Table S1. The gravimetric energy density comparison between graphite anode and auxiliary electrode with Li metal anode.

Utilization of Li (%)	Weight(mg) Li-metal Anode	Total (Including auxiliary electrode)	Gravimetric energy density without Aux-electrode (Wh/Kg)	Gravimetric energy density with Aux-electrode (Wh/Kg)
25%	1.036	7.703□	**589.970**	**493.312**
50%	0.518	7.185	**641.567**	**528.884**
100%	0.259	6.926	**670.904**	**548.661**

Commercial lithium ion batteries	Cathode weight(mg)	Graphite anode weight (mg)	Total (mg)	Gravimetric energy density (Wh/Kg)
1.2	5.405	3.226	8.631	**440.273**

*Fixed capacity of cathode for 1 mAh with NMC622 (average practical capacity ~185 mAh/g, average voltage ~3.8 V.), *Theoretical capacity of graphite is 372 mAh/g, *N/P ratio is capacity ratio of negative to positive electrode

*The mass of the auxiliary electrode was ~1.262 mg, corresponding to the capacity of ~0.472 mAh in Figures S5,*The energy density comparison is simply based on the mass of active materials and assumption that the other components are the same.

Table S2. The volumetric energy density comparison between graphite anode and auxiliary electrode with Li metal anode.

Utilization of Li (%)	Weight(mg)/Volume(cm^3) Li-metal Anode	Total (Including auxiliary electrode)	Volumetric energy density without Aux-electrode (Wh/cm^3)	Volumetric energy density with Aux-electrode (Wh/cm^3)
25%	1.036/0.001901	0.005325□	**0.935**	**0.713**
50%	0.518/0.0009737	0.0043977	**1.211**	**0.864**
100%	0.259/0.0004850	0.003909	**1.435**	**0.972**

Commercial lithium ion batteries	Weight(mg)/Volume(cm^3) cathode	Weight(mg)/Volume(cm^3) graphite	Total Volume (cm^3)	Volumetric energy density (Wh/cm^3)
1.2	5.405/ 0.002162	3.226/0.003226	0.005388 □	**0.705**

*Fixed capacity of cathode for 1 mAh with NMC622 (average practical capacity ~185 mAh/g, average voltage ~3.8 V.). The theoretical capacity of graphite is 372 mAh/g. Tap density of NMC622 is assumed to be 2.5 g/cm^3, while that of graphite is assumed to be 1 g/cm^3. The N/P ratio (capacity ratio of negative to positive electrode) is assumed to be 1.2 for the commercial lithium ion batteries.

*The mass of the auxiliary electrode was ~1.262 mg, corresponding to the additional capacity of ~0.472 mAh in Figures S5. Density of lithium metal is 0.534 g/cm^3.The volumetric energy density comparison is simply based on the mass of active materials and tap density.